Journal of Climate Change
ISSN 2395-7611 Volume 11 (2025) No. 4. pp. 360–374

https://doi.org/10.70917/jcc-2025-025
Article

Multi-Climate Transient Seasonal Analysis of Integrated Solar Assisted Desiccant Indirect Evaporative Cooling System with Dynamic Building Loads

Muzaffar Ali [1,2,*], Suoying HE [3], Fouzia Begum [4], Mohammad Usman [4], Ghulam Qadir Chaudhary [3,5], Mirza Abdullah Rehan [1] and Guiqiang Li [1]

[1] Department of Mechanical Engineering, Faculty of Engineering, Kocaeli University, Turkiye. muzaffar.ali@kocaeli.edu.tr
[2] Department of Energy Engineering, University of Engineering and Technology Taxila, Pakistan, muzaffar.ali@uettaxila.edu.pk
[3] Shandong Engineering Research Centre for High-efficiency Energy Storage and Hydrogen Energy Utilization, School of Nuclear Science, Energy and Power Engineering, Shandong University, Jinan, Shandong 250061, China; s.he@sdu.edu.cn
[4] Department of Mechanical Engineering, University of Engineering and Technology Taxila, Rawalpindi, Punjab,47050 Pakistan; usman.muhammad@uettaxila.edu.pk
[5] Department of Mechanical Engineering, Mirpur University of Science and Technology, Mirpur 10250, AJK, Pakistan; qadir.me@must.edu.pk
* Correspondence author: Muzaffar.ali@kocaeli.edu.tr or Muzaffar.ali@uettaxila.edu.pk

Abstract: Thermal comfort demand in the building sector is increasing remarkably due to population growth, urbanization, and global warming, particularly in hot and humid climates like Pakistan. However, the performance of such systems is strongly influenced by dynamic building loads and transient climate conditions, such as solar irradiance, ambient air temperature, and humidity. This study investigated the adequacy of the solar-assisted desiccant cooler with the Maisotsenko cycle cooler (SADC-Mc) system by performing a transient seasonal analysis for multiple climate zones of Pakistan. The climate zones include humid subtropical (Cwa), Warm semi-arid (BSh), and Warm desert climate (BWh), as exemplified by various cities such as Peshawar, Taxila, Lahore, Multan, and Karachi. Furthermore, the performance of SADC-Mc is also compared with a traditional solar-assisted desiccant cooling system with a direct evaporative cooler (SAD-DEC) in each climate. A detailed solar-assisted desiccant cooling system model was developed in TRNSYS, and a Maisotsenko cycle cooler (M-cycle) EES component model was also incorporated to perform the seasonal (April-September) transient simulation analysis under dynamic building loads for the selected climates. The system model validation findings showed good agreement with published experimental data, with a mean percentage error of 2.7%. The SADC-Mc system was found to be 40-60% more efficient than the traditional desiccant cooling system in terms of COPth for the less humid climates of Taxila, Peshawar, and Lahore. In terms of cooling capacity (CC), the integrated system performed effectively well in all cities, achieving its peak monthly performance in Multan at 5407 kWh. Furthermore, the maximum thermal energy requirement of the SADC-Mc system was reported for Karachi (6603 kWh) in June. In contrast, the SAD-DEC system's thermal energy requirement is almost double (17072 kWh) as compared to the SADC-Mc system. Similarly, the monthly average variation in COP thermal was recorded as ranging from 0.8 to 1.2, along with a total seasonal solar energy gain of 40 MWh for the Taxila climate.

Keywords: solar-assisted cooling; desiccant cooling; different climates; transient analysis; solid desiccant

1. Introduction

Global energy demand and CO_2 emissions have increased significantly, prompting international targets such as those from the EU to increase renewable energy shares and reduce consumption (European Commission, 2006; Banerjee et al., 2016). Since the building sector is a major energy consumer, with air conditioning contributing a substantial share, sustainable alternatives are crucial (Ellis and Mathews, 2002). Solar-driven desiccant cooling systems offer a promising solution by utilizing low-grade heat for dehumidification, which is a significant energy expense in conventional cooling systems (IEA SHC, 2016; Awbi, 2003). Solid desiccant systems—such as those using silica gel or zeolite—are particularly effective because they can be regenerated using solar thermal energy, reducing reliance on electricity and harmful refrigerants (Misha et al., 2012). However, a key challenge limiting wider adoption is performance uncertainty in hot and humid climates, where high moisture levels can strain the system's regeneration capacity (Sahlot and Riffat, 2016). Therefore, determining feasibility at the design stage is essential. This work employs a model-based simulation approach, a well-established method for predicting system performance (Trčka and Hensen, 2010), to evaluate a desiccant cooling system under such demanding conditions.

Solar desiccant evaporative cooling has been widely explored as a viable alternative to conventional vapor-compression air conditioning due to its environmental and economic benefits. For example, a TRNSYS-based study for an institutional building in the subtropical climate of Australia showed that a system with a 10 m^2 solar collector area and a 0.4 m^3 hot-water storage tank achieved a COP_{th} of 0.7 and a solar fraction of 22%, increasing to 1.2 COP_{th} and 69% solar fraction when the collector area was expanded to 20 m^2 and storage to 1.5 m^3 (Baniyounes et al., 2012). A comparative performance evaluation of a solar-driven two-stage rotary desiccant system and a traditional vapor-compression system for Berlin and Shanghai concluded that the desiccant system was more economical and environmentally friendly, meeting cooling demands with regeneration temperatures of 55 °C (Berlin) and 85 °C (Shanghai) and payback periods of 4.7 and 7.2 years, respectively (Ge, Ziegler and Wang, 2010). Likewise, a hybrid air-conditioning system combining a solid desiccant unit with a vapor-compression cycle showed strong suitability for hot and humid climates, using solar energy as the primary source (Jani, Mishra and Sahoo, 2015). A theoretical analysis of a solar cooling system across five regions in Saudi Arabia showed that the thermal COP varied from 0.275 to 0.476 depending on location (Rafique et al., 2016).

The model-based transient simulation approach is well established for such systems. A TRNSYS-based performance analysis of desiccant-based air handling units using solar energy found primary energy savings of 15–24% and CO_2 reductions of 14–22% when using evacuated-tube collectors instead of flat-plate collectors (Angrisani et al., 2016). A TRNSYS and EES study comparing direct/indirect evaporative coolers integrated with desiccant systems concluded that systems with indirect evaporative cooling achieved higher COPs (Elgendy, Mostafa and Fatouh, 2015). A transient simulation for the UAE showed that a recirculation configuration for a desiccant system coupled with an M-cycle dew-point cooler required lower regeneration temperatures and achieved a flow rate of only 1100 m^3/h at peak (Saghafir and Gadalla, 2015).

Other numerical studies on desiccant systems coupled with cross-flow and counter-flow M-Cycle indirect evaporative coolers have shown efficient performance at regeneration temperatures as low as 60 °C (Pandelidis et al., 2016; Pandelidis et al., 2017). For a school building in Adana, Turkey, the monthly average COP_{th} ranged from 0.22 (July) to 0.78 (October), with a seasonal value of 0.43 (Güzelel, Olmus and Büyükalaca, 2022). Experimental evaluation of a solid desiccant system integrated with a cross-flow M-Cycle cooler demonstrated 60–65% higher efficiency than a conventional SAD-DEC configuration (Kashif et al., 2018). Another experimental study using a solar-assisted desiccant system with an M-Cycle cooler achieved a COP of 0.91, a cooling capacity of 3.78 kW, and a 70% solar fraction (Chaudhary et al., 2018). Additionally, modern AI-based techniques have been applied for performance optimization of desiccant-evaporative systems (Tariq et al., 2023).

Based on the above literature review, it is evident that climate and operating conditions significantly impact the performance of solar-assisted cooling systems. However, transient seasonal analysis of the proposed integrated system, SADC-Mc, has rarely been investigated for multiple climate zones. Therefore, to have a comprehensive study, three climates were selected because they involved a wide

range of climate variation by representing five different cities with variable solar radiation, including a humid subtropical climate (Taxila), a warm semi-arid climate (Peshawar and Lahore), and a warm desert climate (Multan and Karachi). Additionally, model-based transient simulations were crucial at the initial design stage to determine the feasibility of such systems. Therefore, in this study, a model-based simulation approach was implemented to analyze dynamic building loads and various humid subtropical climates in Pakistan, coupling TRNSYS with EES for a detailed thermal analysis of a solar-assisted desiccant system integrated with an M-Cycle evaporative cooling system. Finally, a comparative study was also conducted with a conventional system to highlight the potential advantages of the Maisotsenko cycle-based indirect evaporative cooling system.

2. Description of the Integrated System

In the current work, a solar-assisted desiccant cooling system integrated with the Maisotsenko cycle indirect evaporative cooling system (SADC-Mc) was investigated for its performance in various climates. Compared to conventional indirect evaporative cooling, the M-cycle indirect evaporative cooler can cool the product air down to the dewpoint temperature of the air. This component consisted of multiple dry and wet channels. Air enters the dry channels and is cooled as it moves through them, rejecting heat to adjacent wet channels that undergo evaporative cooling. The integrated solar desiccant evaporative cooling system was comprised of a desiccant wheel (DW), a heat wheel (HW), an M-cycle cooler on the process side, and a direct evaporative cooler on the regeneration side, as shown in Figure 1. In ventilated recirculation, pre-mixed air was first introduced into the process side of the DW, where it was dehumidified and its temperature was raised (Points 1-2). It then entered HW for sensible pre-cooling at the process side, rejecting its heat to the return side air stream (Point 2-3). Later, this air entered the M-cycle evaporative cooler, where it was further cooled without adding moisture (Point 3-4) and finally supplied to the air conditioning space. On the other hand, the ambient air was provided to the direct evaporative cooler on the regeneration side (Point 5-6), where it was cooled to increase the cooling effectiveness of HW (Point 6-7). Solar evacuated tube collectors supplied the heat required for desiccant regeneration through an air-water heat exchanger (Points 7-8). In the event of a night or a cloudy day, the regeneration demand was met by a storage tank coupled with an auxiliary heat source. Moreover, in the current work, to increase the cooling capacity of the system, the standard ventilation cycle was modified as a recirculated ventilation desiccant air-cooling cycle. In this cycle, return air from the room (60%) was recirculated and mixed with 40% ambient air as process air. This was because approximately 40% of the air is exhausted as working air in the M-Cycle cooler. Therefore, approximately 10-40% of outdoor fresh air was added as ventilation air, as required in commercial and institutional buildings. Such a system was called the "ventilated recirculation" configuration. In contrast, 100% ambient air was used on the regeneration side.

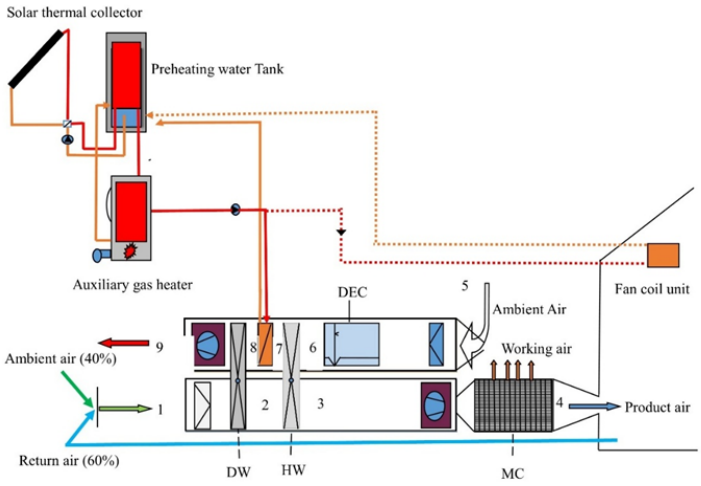

Figure 1. Schematic representation of SADC-Mc: Ventilated-Recirculation Configuration.

3. Model Development and Transient Simulation

In this study, the proposed system configuration was modelled and simulated in TRNSYS 18 to check the performance of the cooling system in different climate zones, including Peshawar (34.1°N, 71.5°E),

Taxila (33.7°N, 72.8°E), Lahore (31.5°N, 74.3°E), Multan (30.1°N, 71.5°E) and Karachi (24.8°N, 67.1°E) of Pakistan. Weather data were used from the meteorological data of TMY files. A solar-assisted desiccant system was modelled in TRNSYS along with a building thermal loads model, and the M-cycle (Mc) model was developed in EES. Afterwards, the sub-models were integrated (SADC-Mc) by coupling EES with TRNSYS to check the behaviour of the proposed configuration for transient analysis. A comparison of the SADC-Mc system with the conventional desiccant evaporative cooling system (SAD-DEC) model was conducted for each climate. As the purpose of this study was to analyse the energy performance of the SADC-Mc system in different climates, simplifying assumptions were made in the TRNSYS modelling and simulation, including energy losses in the connected piping and/or valves, which were ignored, and the performance analysis was carried out considering similar building dynamic cooling loads as represented in Section 4.

3.1. Simulation assumptions and justification

The following assumptions are taken for this study.

Piping and Duct Losses: Heat gains and losses in all connecting piping and ducts were neglected. As the piping and ducts are modelled assuming the industry standard insulation, where the marginal energy loss impact is less than 2-3%. It was considered negligible for this comparative system analysis, resulting in a significant reduction of model complexity without compromising the validity of comparative results.

Quasi-Steady State Components: The desiccant wheel, heat exchangers, and M-cycle unit are simulated using performance maps, assuming quasi-steady-state operation at each timestep, as the thermal mass of these components is small relative to the system's dynamics.

Ideal Control Operation: The system controllers for pumps, motors, and fans are assumed and modelled with perfect sensing and instantaneous actuation, neglecting real-world hysteresis and delay.

Air leakage and auxiliary heating: For simplicity of analysis, it is assumed that the air ducts are perfectly sealed and insulated, and that there is no air leakage or auxiliary heating of the ducts.

Constant Internal Loads: Internal heat gains from occupants and equipment were defined using standardized schedules rather than stochastic variations, as the use of consistent, scheduled profiles is the established method for whole-building energy.

3.2. Building Thermal Load Model Development

An office building was considered, whose 3D model was developed in Google SketchUp and exported to the TRNSYS simulation studio for building thermal loads calculations over a six-month period. The typical single-story building in Pakistan comprises four (04) zones along with a storeroom and washrooms. These zones were labelled along with area and volume sizes as; general managers room (GMR A = 15.5 m^2, V = 55 m^3), meeting room (MR A = 44 m^2, V = 160 m^3) that was also an office room 3 (O3) for the 10 people, office 1 (O1 A = 16 m^2, V=58 m^3) and office 2 (O_2 A = 13 m^2, V = 47.5 m^3). The dotted green line points south, and the solid red line points east. MR's external wall was facing South, and offices O1 and O2's external walls were facing East, while GMR's external wall was facing West in this building model, as shown in Figure 2.

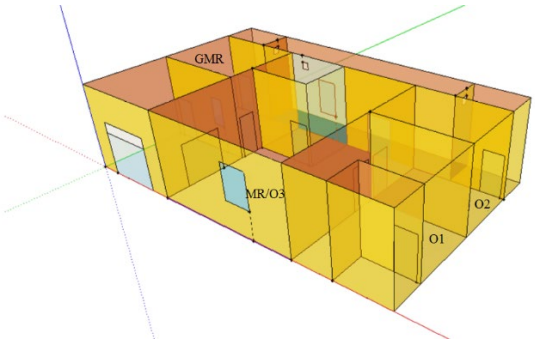

Figure 2. Building model developed in Google SketchUp.

The building envelope properties of each zone were defined in the TRNBuild program. All surfaces, including walls, windows, roof, and floor, were described in layers according to local construction practice. The details of the construction walls used in the building envelope are given in Table 1. The materials of layers 1 and 2 in the walls were brick and Polyurethane (insulation), respectively. Whereas layer 1 was RCC1 and clinker for the roof. Regarding the construction of windows in zones, ASH140 DBLE – MOD was used, which was a double-glazing window with 3.1 mm thickness of each glass and

an Aluminium frame. The area and overall heat transfer coefficient values for windows were: GMR- A_{wind} = 0.74 m^2, MR- A_{wind} = 1.86 m^2, U = 2.88 W/ m^2.K). 17 people occupied the office from 9:00 a.m. to 5:00 p.m., and lighting was provided simultaneously. The infiltration and heating/cooling setpoints were set as input from the TRNSYS simulation studio.

Table 1. Building wall specifications.

Wall type	Layer 1 thickness (m)	Layer 1 thickness(m)	Total thickness (m)	U-value ($W/m^2.K$)
Boundary	0.227	0.001	0.228	0.728
External	0.227	0.001	0.228	0.728
Adjacent	0.227	0.001	0.228	0.728
Roof	0.253	0.001	0.254	2.46

3.3. Solar Thermal System Model Development

In the current system model, a solar-assisted water heating system (SWHS), which consisted of evacuated tube collectors, was employed to meet the regeneration heat requirement of the desiccant wheel. The pump control signal was generated using a Calculator (equation 2), and it operated the pump only when both the season schedule (Type 515) and the pump schedule (Type 14b) signals were 1. A single-speed pump (Type 114) was used to pump the mixture (water + ethylene glycol) from 9:00 a.m. to 5:00 p.m. The differential controller (Type 2 b) allowed the water to move from the storage tank to the solar collector when ΔT was at its minimum value of 5°C. Evacuated tube solar collectors (Type 71) heated the mixture, which was then linked to the stratified storage tank (Type 4c). The heated mixture passed through the Tee-piece (Type 11h), where it was mixed with the cold stream (if needed), and then further heated up to the set point temperature (if required) by the auxiliary heater Type 700. Heated water from the heater entered the bypass-fraction heating coil (Type 753A), then flowed into the air-water heat exchanger. Finally, after heating the regeneration air, it then entered the tempering valve Type 11 and completed the cycle. A few key components and their corresponding TRNSYS types, along with their design values, are listed in Table 2.

3.4. Integrated System Model Development

In this study, a desiccant evaporative cooling system integrated with M-cycle was modelled in a ventilated-recirculated configuration. Key design parameters of the desiccant wheel, air-to-air heat exchanger, and evaporative cooler were provided in Table 2. Air properties were obtained from the standard format weather data file (TMY) Type 15 for the selected cities. In the developed model, Type 648 served as the mixer, blending 40% ambient air and 60% return air to achieve a 100% air mixture for the desiccant system. The building's thermal loads (cooling and heating) were incorporated through the Excel input file Type 62. Calculator (Equ-1) was used to calculate the mass flow rate for varying cooling loads. The humidity set point in the desiccant wheel was 0.007kg/kg. Initially, air was allowed to enter the desiccant wheel DW (Type 683) process side for dehumidification purposes. Air, after passing through the Desiccant wheel, dehumidifies, and its temperature increases. It was then passed through the process side of the air-air heat exchanger heat wheel (Type 760b), where it exchanged heat with the cold stream coming from a direct evaporative cooler (DEC) on the regeneration side.

Another model of a conventional desiccant cooling system (SAD-DEC) was also developed for comparative analysis and comparison with SADC-Mc. It uses a direct evaporative cooler instead of the M-cycle cooler on the process side. All other design, climate, and operating conditions were kept the same. The subsystem models were integrated into a single system model. Still, building loads were dealt with separately in Building Wizard (upper block) and inserted as an Excel file named (building loads) in the SADC-Mc system (lower block) in Figure 3. The upper block represented the building dynamic load model in which building envelope details, schedules, number of occupants, lightning, infiltration, and heating and cooling were defined in TRNBuild. Then, all setpoints were defined as inputs from the TRNSYS simulation studio through the building model Type 690 (lower block).

Table 2. Design parameters and TRNSYS -Type of the system.

Component/Type	Parameter	Value
Solar collector/Type-71	Efficiency	0.68 (z1 = 1.96, z2 = 0.027)
	Area	40 m^2
Flow pump/ Type-114	Flow rate	767 kg/hr
	Max. Power	200 W
Storage tank/Type 4c	Volume	$4m^3$
	Loss coefficient	2.5 kJ/hr.m^2.K
Weather/ Type 15-2	---	---
Desiccant wheel/ Type683	Efficiency	F1: 0.09, F2: 0.76
	Air flow rate	0.35-0.96 kg/s
Heat wheel/ Type 760b	Sensible effectiveness	0.60
Evaporative cooler/ Type 506	Saturation efficiency	0.85

Therefore, the complete building dynamic load profile is integrated through Type 690 during the simulation of the system model. The developed component model of the MC cooler was based on the experimental data and was called in the transient simulation via calling the EES routine Type 66. This program received dynamic inputs at discrete intervals, known as the EES program.

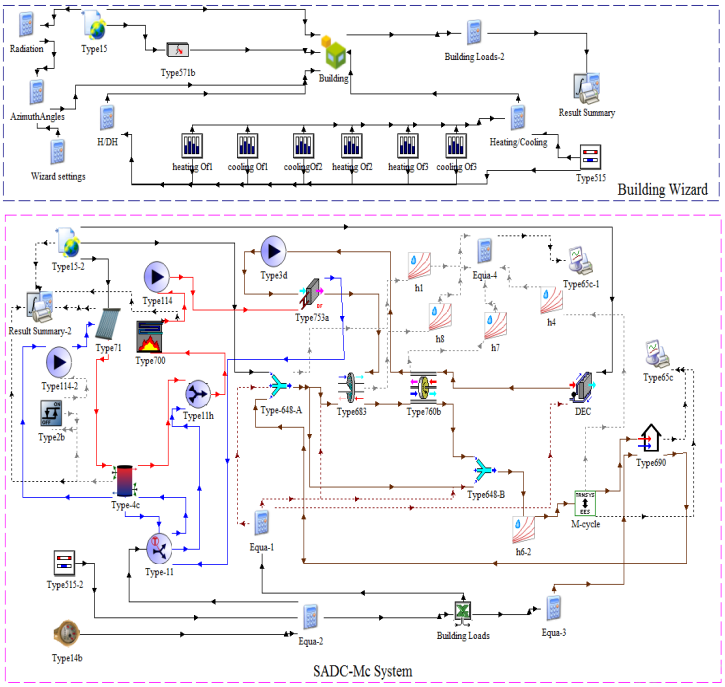

Figure 3. TRNSYS model of solar-assisted desiccant cooling system integrated with M-cycle (SADC-Mc).

4. Results and Discussion

The performance of the solar-assisted desiccant evaporative cooling system integrated with the M-cycle (SADC-Mc) was significantly influenced by ambient conditions, as it involved the evaporation process and solar radiation collection. The current study was focused on a detailed investigation of the system performance in different climate zones of Pakistan. Peshawar, Taxila, Lahore, Multan, and Karachi were chosen as geographical locations for systems performance analysis. Data on ambient conditions were obtained from the TMY files for each climate. Köppen climate zone classification (KCZC) was used to divide the climates of selected cities into different categories as presented in Figure 4 (Peel, Finlayson and McMahon, 2007). In this classification, world climates were divided into five

groups, designated as A, B, C, D, and E, with each major group further subdivided into subtypes, such as Af, Am, and Aw. The chosen cities are encircled in Figure 4, which depicts the Pakistan map using the Köppen climate classification.

The climate conditions were considered in terms of ambient dry bulb temperature, ambient relative humidity, and global solar radiation for the selected cities during the summer season, from April to September, with 8 hours (9 am to 5 pm). Figure 5(a) illustrates the dynamic air-conditioning loads of the building, where sensible and latent loads are displayed separately. It can be observed from this Figure that the maximum sensible cooling load of the building occurs at a time step of 5000 hours, which corresponds to July. It is also evident that the maximum latent air-conditioning load occurs in this month, as it is characterised as the hottest and humid month in Pakistan's climate. Figure 5(a) further highlights that cooling demand exists only from April to September. In comparison, Figures 5(b) and 5(c) depict the average ambient air temperature and absolute humidity for six-month periods (April-September) of five chosen climates. The temperature varied from 27 °C to 39°C, with the maximum value recorded in Multan city during the hottest month of June. It was observed that Peshawar, Taxila, and Lahore also have average high temperatures during June. In comparison, Karachi has a bit different temperature profile; it has the lowest average ambient air temperatures during the entire period, but the highest mean ambient absolute humidity for the same summer season. The key reason is that Karachi is situated at the southern tip of the country, along the Arabian Sea coast; therefore, the city experiences a tropical climate, characterized by mild and dry winters and hot, humid summers. It was also observed that the average absolute ambient humidity exhibited a similar increasing trend for the three cities: Taxila, Lahore, and Multan. Overall average absolute humidity in Karachi was the highest, ranging from 17 to 21.5 g/kg.

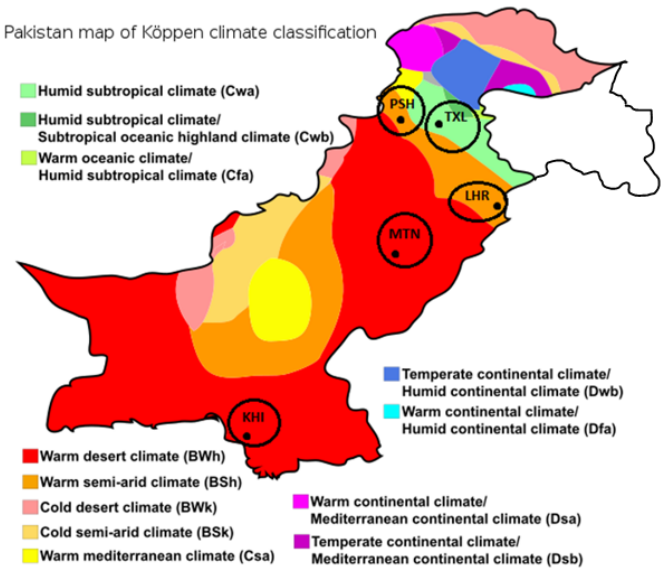

Figure 4. Köppen climate classification for Pakistan.

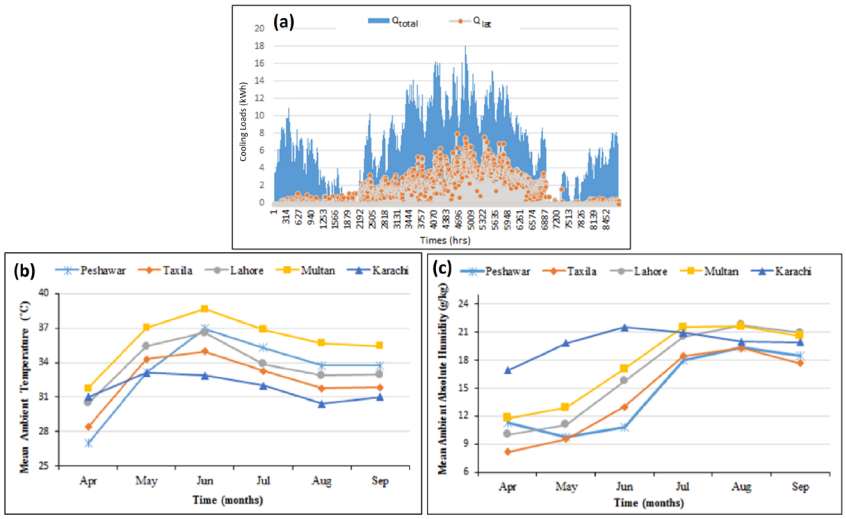

Figure 5. (**a**): Annual building dynamic loads (**b**,**c**): Monthly average ambient temperature, absolute humidity of different climate zones.

4.1. The system model validation

The developed model at the system level was validated with the published data (Chaudhary, 2018, page 696) against the same parameters (air flow rate 660kg/hr, inlet air temperature 25-45 °C, humidity ratio 14 g/kg, return air conditions of 27 °C, 12.5g/kg, and regeneration temperature of 70 °C). Figure 6 (a)-(b) shows that the model-based performance in terms of supply air temperature and supply air humidity ratio of the SADC-Mc system is in good agreement with the published experimental data, with a mean percentage deviation of 2.7% due to thermal losses.

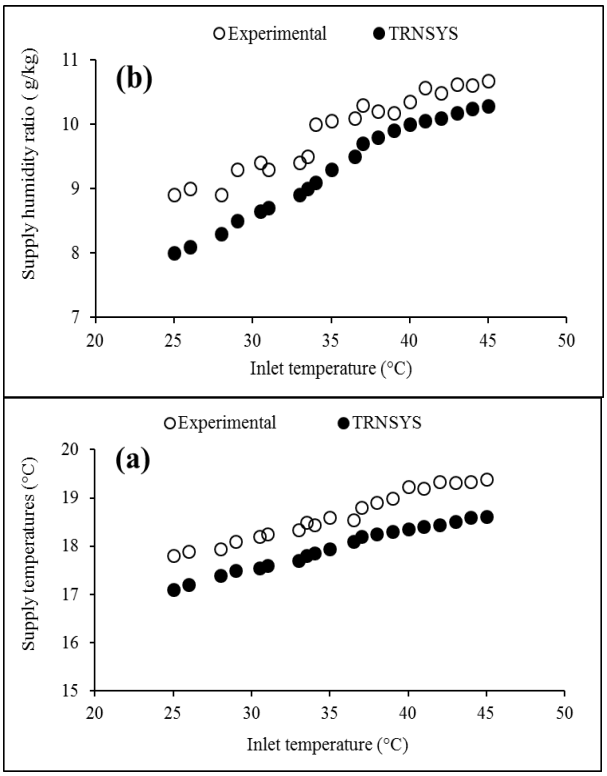

Figure 6. The model validation based on: (**a**) supply air temperature, (**b**) supply air humidity ratio.

4.2. Transient analysis of SADC-Mc and the SAD-DEC in various climates

Cooling capacity (CC) indicates the cooling load that the system can handle. It was measured from the product of the overall air temperature reduction and the air mass flow rate, as shown in Figure 7. It can be observed that the cooling capacity of the SAD-DEC system was usually higher than that of the SADC-Mc system, because 40% of the process air flow was diverted towards wet channels (working air) in the M-cycle, and only 60% of the flow is supplied to the building. This effect is evident in the analysis of Taxila and Peshawar. Subtropical conditions characterise these climates. The airflow rates for both systems were maintained to achieve a comfortable temperature range of 24-26 °C in the building. However, the cooling capacity of the SADC-Mc system for Lahore, Multan, and Karachi was higher than the SAD-DEC cooling capacity. The reason is that these climates are characterized as hot and humid, and the performance of SADC-Mc is superior in terms of cooling capacity for such climates. The upsurge in ambient temperature, along with the absolute humidity level, negatively affects the regeneration air, as it is less cooled and exchanges less heat with the process air through the air-to-air heat exchanger, which in turn produces less ΔT between the process inlet and supply outlet. The effect was more evident for SAD-DEC systems as their cooling effectiveness was limited to the wet bulb temperature of incoming process air.

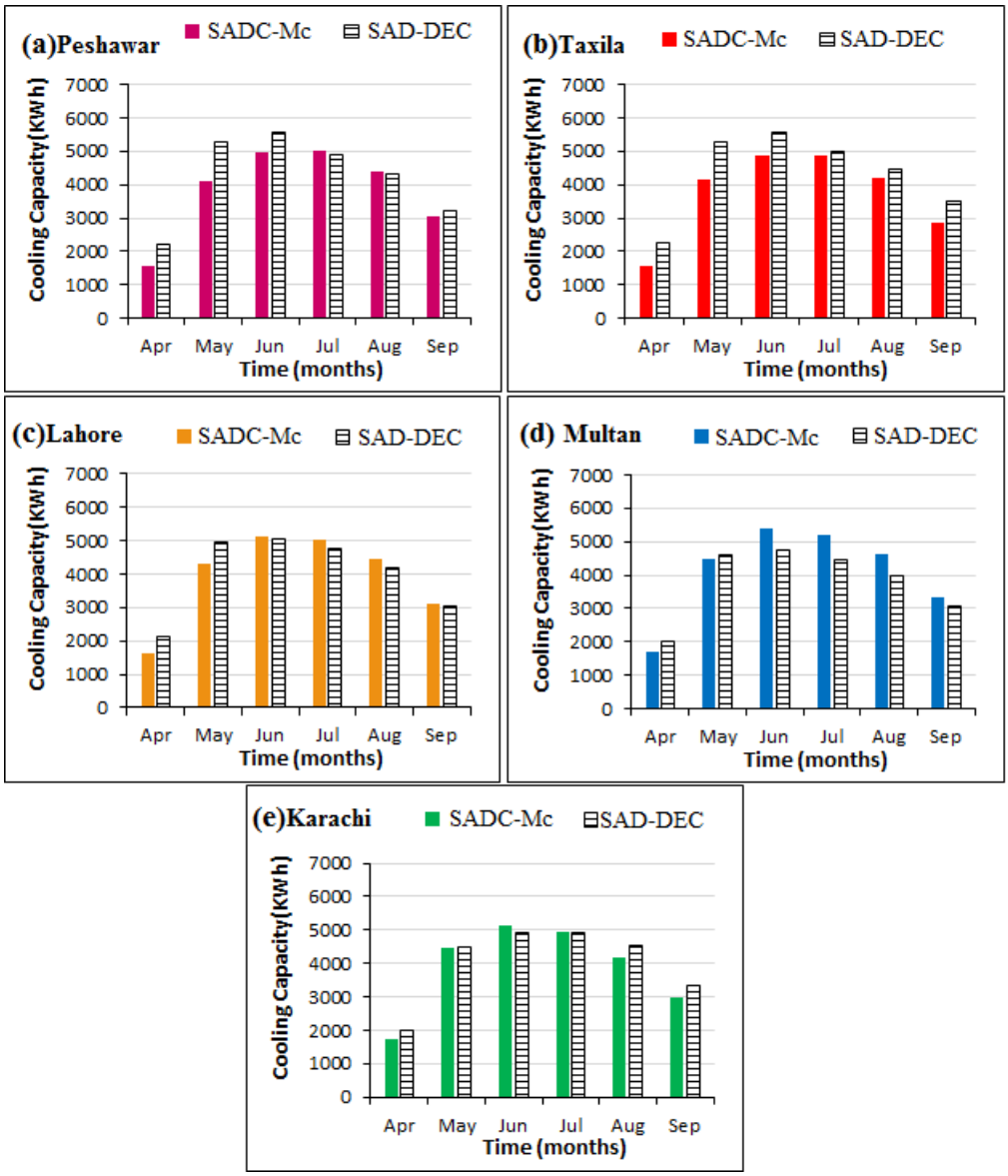

Figure 7. Variation in cooling capacity of both systems for different climate zones.

The SADC-Mc system performed well in this situation to cope with the required comfort demand, as the humidity set points were 7g/kg, and the process air coming out of the desiccant wheel was less hot

than the SAD-DEC system's process air. Moreover, the effectiveness of the M-cycle cooler was up to the dewpoint temperature, which increased the cooling capacity of the SADC-Mc system. SADC-Mc cooling capacity was highest in June, when air temperatures peaked for each climate. However, the SAD-DEC system cooling capacity was also high when the ambient temperature and humidity ratio were not so high. The highest cooling capacity achieved was 5569 kWh via SAD-DEC for the climate of Peshawar in June. Moreover, the regeneration demand of the system increased as the outside humidity levels rose, causing a higher latent load, as shown in Figure 8. Highly humid ambient air caused higher regeneration air inlet absolute humidity, which in turn intensified the demand for desiccant wheel moisture removal. In June, the ambient humidity ratio of each climate was the highest, as was the SAD-DEC regeneration demand. Moreover, Karachi has the highest absolute humidity throughout six months, which is why it had higher regeneration demand, and for other climates, the trend is somewhat the same. Furthermore, high ambient temperature negatively affected the desiccant wheel performance and, in turn, elevated the regeneration demand, e.g., in Multan.

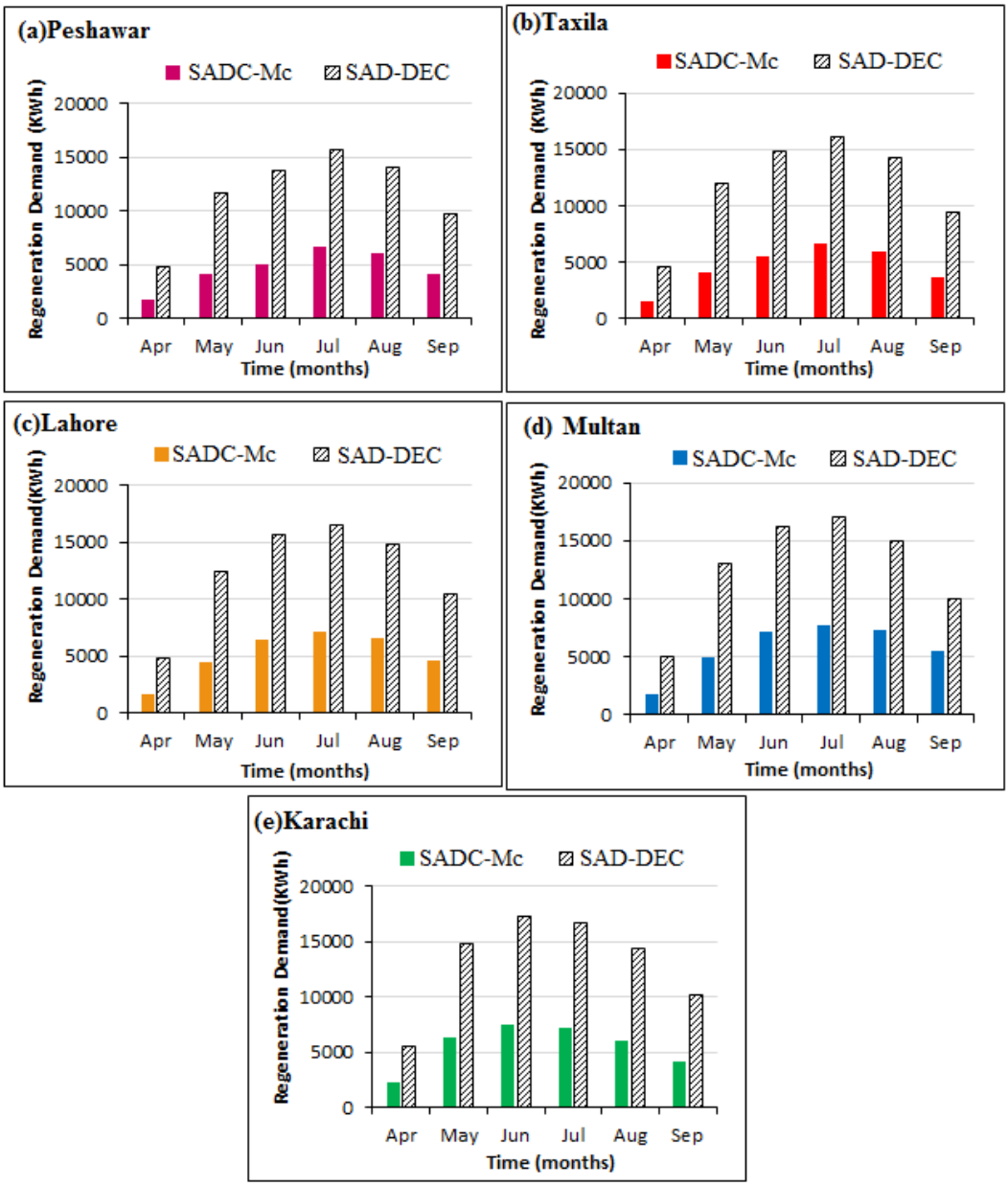

Figure 8. Comparison of the regeneration heat demand with time for different climates.

A comparison of dehumidification is presented in Figure 9, primarily to evaluate the performance of the desiccant system. The dehumidification effectiveness of the SAD-DEC system is overall higher, corresponding to the same regeneration temperature for both systems, because only 10% ambient air is

added to the SAD-DEC, as compared to 40% for the SADC-Mc, and the remaining air is recirculated from the room. Building latent loads are assumed to be the same for all cities; therefore, the dehumidification effect is not as variable in SAD-DEC. However, for the SADC-Mc system, as 40% of the ambient air is allowed to enter the desiccant wheel to fulfil the CFM requirement and cope with both cooling and ventilation demands, the dehumidification effect is apparent. Dehumidification follows the same trend as that of ambient humidity ratios for all cities. The highest dehumidification effect is observed in Karachi and Multan, where ambient humidity reaches up to 21-22g/kg.

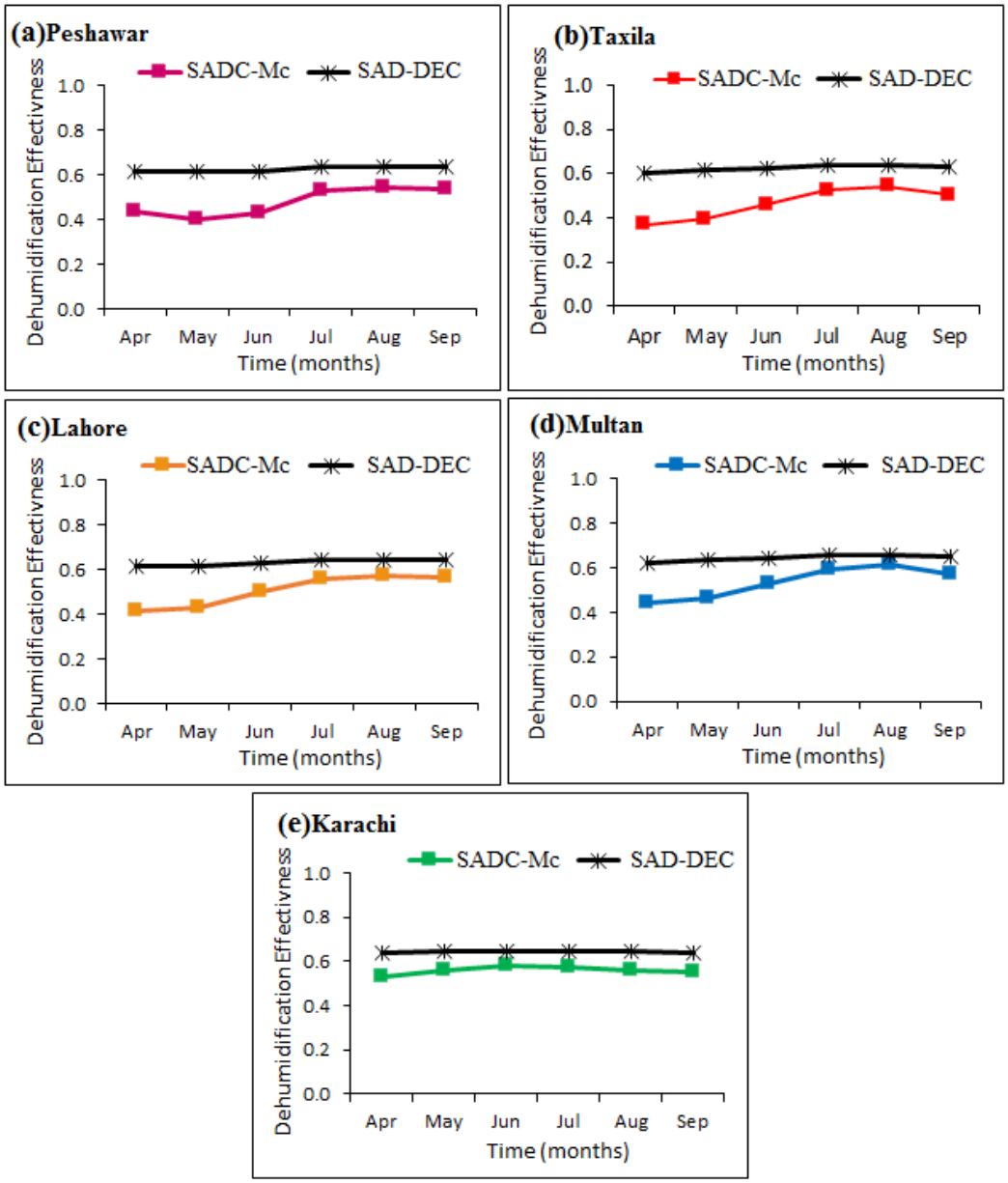

Figure 9. Variation of dehumidification Effectiveness with time.

The thermal coefficient of performance (COP_{th}) was strongly linked with the cooling capacity and regeneration heat demand. It can be seen from Figure 10 that COP_{th} for Karachi was the lowest among all climates. This is because Karachi belongs to a warm desert climate characterized by a temperature range of 29-35 °C and a humidity ratio ranging from 15-21 g/kg. As the ambient temperatures are low and humidity is high, the cooling capacity of SADC-Mc is reduced that results in lower $COP_{th.}$ due to low inlet air temperatures and high humidity, which adversely affected the dew point effectiveness of the SADC-Mc, resulting in low system performance. The highest COP_{th} of 1.16 was observed in April for the Taxila climate, with an inlet air temperature of 29 °C and an absolute humidity of 8 g/kg. The overall COPth trend for all months was maximum for the Taxila climate, ranging between 0.72 and 1.16. Moreover, the COP_{th} of the SADC-Mc system was higher than the conventional system due to enhanced

cooling (dew point) effectiveness caused by the M-cycle indirect evaporator.

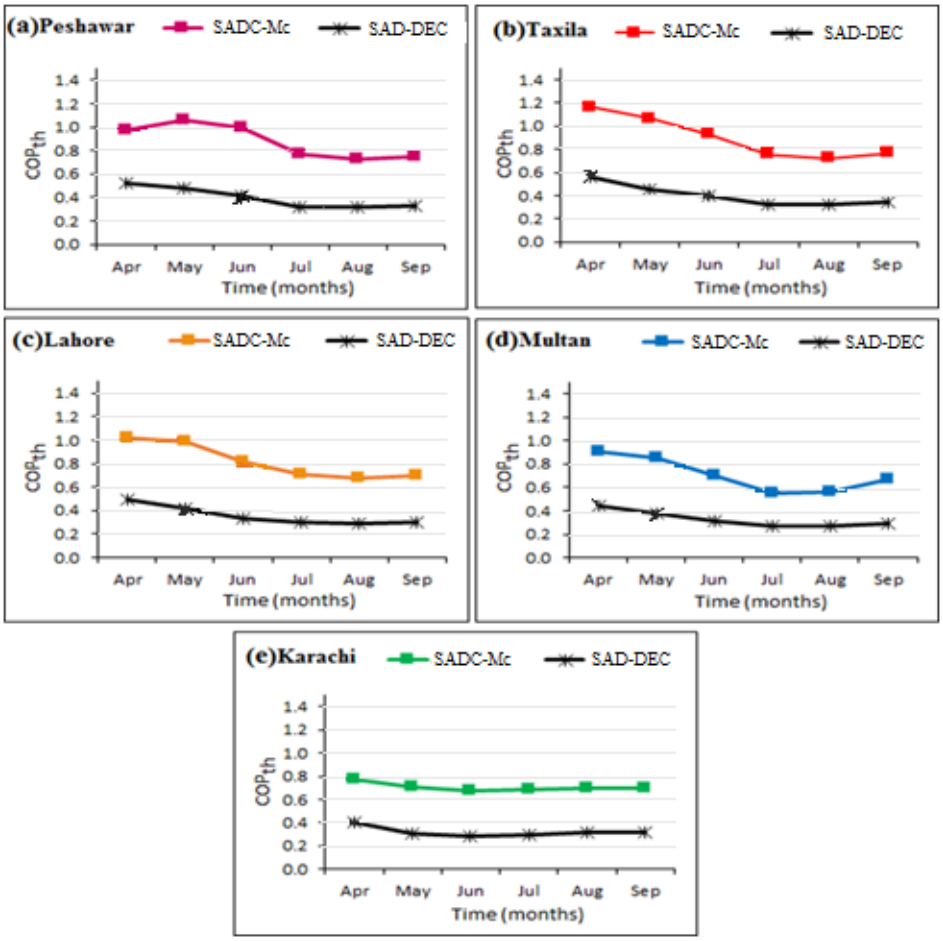

Figure 10. Performance comparison in terms of COP_{th} for different climate zones.

Figure 11 shows the collector efficiency for both cooling systems along with the effect of solar radiation in each city. The highest possible efficiency achieved is in Peshawar in June, when Q_{req} is 13829 kWh, and the mean ambient conditions are (36.9 °C, 10.79 g/kg) with the mean instantaneous solar radiation of 676 W/m^2. Solar loop attached to SAD-DEC achieves the highest efficiency from April to June due to higher dehumidification demands and the requirement of handling high latent loads. In contrast, SADC-Mc was exposed to limited latent loads, and its thermal energy utilization was also low, resulting in low collector efficiency attached to this system. However, from July to September, the collector thermal efficiency of both systems remained almost similar due to the full utilization of solar thermal energy for both systems. Moreover, it is also evident that the highest incident solar radiation occurs in Peshawar, along with the best collector performance in the same city for both cooling systems in terms of collector efficiency.

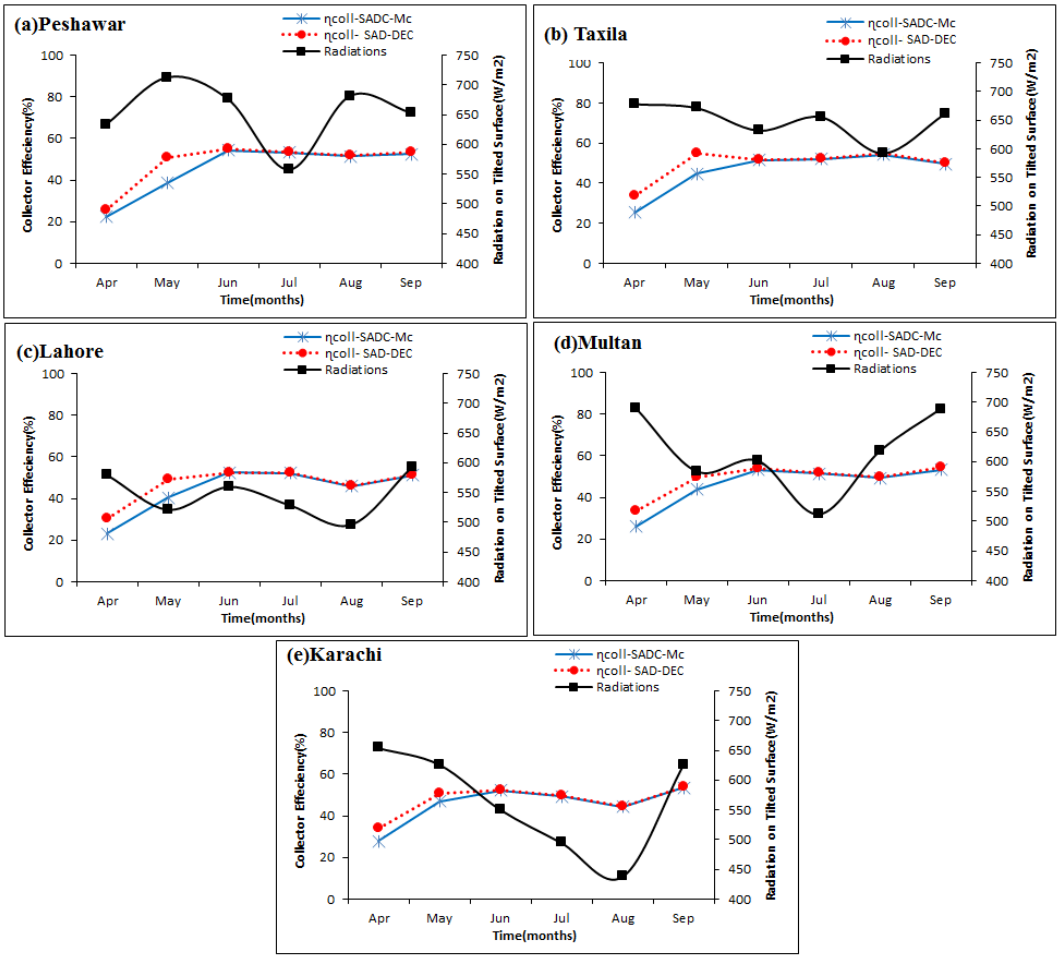

Figure 11. Collector Efficiency Variation along with Solar Radiation.

5. Conclusion

This study focused on a detailed transient seasonal analysis of a solar-assisted desiccant air-cooling system integrated with an M-cycle indirect evaporator (SADC-Mc) under dynamic building loads in multiple climates. A comprehensive model of the integrated system was developed in TRNSYS, including a solar thermal system, a building load model, and a desiccant cooling system. A comparative analysis of a solar-integrated system with a conventional desiccant evaporative cooling (SAD-DEC) system was also performed. The system model validation was found to be in good agreement with published experimental data, with a mean percentage deviation of 2.7%. The results revealed that the SADC-Mc system was 40-60% more efficient than the conventional SAD-DEC system in terms of COP_{th} for the less humid climates of Taxila, Peshawar, and Lahore. The SADC-Mc system achieved a promising cooling capacity for all climates, with the highest value in June, corresponding to 5407 kWh in Multan, compared to 4700 kWh for SAD-DEC. Furthermore, the maximum Q_{req} of the SADC-Mc system was reported for Karachi (6,603 kWh) in June, whereas the Q_{req} of the SAD-DEC system was more than double (17,072 kWh) that of the SADC-Mc system in June. Moreover, the average seasonal collector efficiency was highest in Taxila, corresponding to 59%. Ultimately, it was evident that the SADC-Mc system proved to be an efficient and sustainable alternative to the conventional direct evaporative cooling system, suitable for various climate zones, thereby achieving the desired level of human thermal comfort in buildings.

However, real-world implementation of the SADC-Mc system must carefully consider local climate conditions, particularly solar irradiation availability, to ensure adequate system sizing and solar fraction for economic viability. While the system offers significant operational savings, the high initial investment for solar thermal components and the M-cycle cooler presents a key challenge for widespread adoption. Therefore, feasibility studies incorporating lifecycle cost analysis and potential government incentives are crucial for different regions. Strategic implementation should prioritize areas with high solar resources and high electricity costs to maximize return on investment and accelerate market penetration.

Author Contributions
Muzaffar Ali: Conceptualization, writing – review & editing. Suoying HE: visualization, validation, formal analysis, data curation. Fouzia Bibi: Writing, formal analysis, investigation. Muhammad Usman: Investigation and review of formal analysis. Ghulam Qadir Chaudhary: Writing – review & editing. Mirza Abdullah Rehan: Software, validation of model. Guiqiang Li: Review & editing. All authors have read and agreed to the published version of the manuscript.

Conflict of Interest
The authors declare that there is no conflict of interest amongst the authors.

Data Availability
The data is available on the request.

Nomenclature

CFC	Chlorofluorocarbon	-
COP	Coefficient of performance	-
DEC	Direct evaporative cooler	-
DW	Desiccant wheel	W/m^2
HW	Heat wheel	-
IEC	Indirect evaporative cooler	-
Mc	Maisotsenko Cycle	-
Q	Thermal energy	kW
Q_{sol}	Solar thermal energy	kW
RMSE	Root mean square error	-
SADC-Mc	Solar-assisted desiccant cooler with the Maisotsenko cycle	-
SAD-DEC	Traditional solar-assisted desiccant cooling system with a direct evaporative cooler	-
SWHS	Solar water heating system	-
T	Temperature	°C
T_{amb}	Ambient temperature	°C
Greek Letters		
η	Efficiency	%
Subscripts		
coll	collector	
d	demand	
in	inlet	
lat	latent	
out	outlet	
req	required	
sen	sensible	
th	thermal	
total	Total	

References

Angrisani, G., Roselli, C., Sasso, M., Tariello, F. & Vanoli, G.P., 2016. Performance assessment of a solar-assisted desiccant-based air handling unit considering different scenarios. *Energies*, 9(9), p.724.

Awbi, H.B., 2003. Ventilation of buildings. *International Journal of Ventilation*, 2(3), pp.287–289.

Baniyounes, A.M., Liu, G., Rasul, M.G. & Khan, M.M.K., 2012. Analysis of solar desiccant cooling system for an institutional building in subtropical Queensland, *Australia. Renewable and Sustainable Energy Reviews*, 16(8), pp.6423–6431.

Banerjee, S.G., Moreno, A., Sinton, J., Primiani, T. & Seong, J., 2016. Regulatory Indicators for Sustainable Energy: A Global Scorecard for Policy Makers. Washington, DC: International Bank for Reconstruction and Development / World Bank.

Chaudhary, G.Q., Ali, M., Sheikh, N., Gilani, S. & Khushnood, S., 2018. Integration of solar-assisted solid desiccant cooling system with efficient evaporative cooling technique for separate load handling. *Applied Thermal Engineering*, 140, pp.696–706.

Elgendy, E., Mostafa, A. & Fatouh, M., 2015. Performance enhancement of a desiccant evaporative cooling system using direct/indirect evaporative cooler. *International Journal of Refrigeration*, 51, pp.77–87.

Ellis, M.W. & Mathews, E.H., 2002. Needs and trends in building and HVAC system design tools. *Building and Environment*, 37(5), pp.461–470.

European Commission, 2006. Green Paper: European Strategy for Sustainable, Competitive and Secure Energy. *COM* (2006) 105, pp.1–20.

Ge, T.S., Ziegler, F. & Wang, R.Z., 2010. Performance comparison between a solar-driven rotary desiccant cooling system and conventional vapor compression system. *Applied Thermal Engineering*, 30(6–7), pp.724–731.

Güzelel, Y.E., Olmus, U. & Büyükalaca, O., 2022. Simulation of a desiccant air-conditioning system integrated with dew-point indirect evaporative cooler for a school building. *Applied Thermal Engineering*, 217, 119233.

IEA SHC, 2016. Solar Heating and Cooling Technology Collaboration Programme Annual Report. pp. 2–84.

Jani, D.B., Mishra, M. & Sahoo, P.K., 2015. Performance studies of hybrid solid desiccant–vapor compression air-conditioning system for hot and humid climates. *Energy and Buildings*, 102, pp.284–292.

Kashif, S.M., Chaudhary, G.Q., Ali, M., Sheikh, N.A., Khalil, M.S. & Ahmed, N., 2018. Experimental evaluation of a solid desiccant system integrated with cross-flow Maisotsenko cycle evaporative cooler. *Applied Thermal Engineering*, 128, pp.1476–1487.

Misha, S., Mat, S., Ruslan, M.H. & Sopian, K., 2012. Review of solid/liquid desiccant in drying applications and regeneration methods. *Renewable and Sustainable Energy Reviews*, 16(7), pp.4686–4707.

Pandelidis, D., Anisimov, S., Worek, W.M. & Drąg, P., 2016. Numerical analysis of a desiccant system with cross-flow Maisotsenko cycle heat and mass exchanger. *Energy and Buildings*, 123, pp.136–150.

Pandelidis, D., Anisimov, S., Worek, W.M. & Drąg, P., 2017. Analysis of different applications of Maisotsenko cycle heat exchanger in desiccant air-conditioning systems. *Energy and Buildings*, 140, pp.154–170.

Peel, M.C., Finlayson, B.L. & McMahon, T.A., 2007. Updated world map of the Köppen–Geiger climate classification. *Hydrology and Earth System Sciences*, 11, pp.1633–1644.

Rafique, M.M., Rehman, S., Lashin, A. & Al-Arifi, N., 2016. Analysis of a solar cooling system for climatic conditions of five different cities of Saudi Arabia. *Energies*, 9(2), pp.1–13.

Saghafir, M. & Gadalla, M., 2015. Solid desiccant air-conditioning system using Maisotsenko cooling cycle in UAE. In: Proceedings of the Third International Conference on Water, Energy and Environment (ICWEE), Sharjah, UAE.

Sahlot, M. & Riffat, S.B., 2016. Desiccant cooling systems: A review. *International Journal of Low-Carbon Technologies*, 11(4), pp.489–505.

Tariq, R., Ali, M., Sheikh, N.A., Shahzad, M.W. & Xu, B.B., 2023. Deep learning artificial intelligence framework for sustainable desiccant air-conditioning system: Optimization toward reduction in water footprints. *International Communications in Heat and Mass Transfer*, 140, 106538.

Trčka, M. & Hensen, J.L.M., 2010. Overview of HVAC system simulation. Automation in Construction, 19(2), pp.93–99.Peel M. C., Finlayson B. L., McMahon T. A., 2007. Updated World Map of the Köppen-Geiger Climate Classification Updated world map of the Köppen-Geiger climate classification. *Hydrol. Earth Syst. Sci.*, vol 11, pp. 1633–1644.